Search for charginos nearly mass degenerate with the lightest neutralino in e^+e^- collisions at centre-of-mass energies up to 209 GeV

A. Heister, S. Schael, R. Barate, R. Bruneliere, I. de Bonis, D. Decamp, C. Goy, S. Jezequel, J P. Lees, F. Martin, et al.

ORGANISATION EUROPÉENNE POUR LA RECHERCHE NUCLÉAIRE (CERN)
Laboratoire Européen pour la Physique des Particules

CERN-EP/2002-020
8 March 2002

Search for charginos nearly mass degenerate with the lightest neutralino in e^+e^- collisions at centre-of-mass energies up to 209 GeV

The ALEPH Collaboration*)

Abstract

A search for charginos nearly mass degenerate with the lightest neutralino is performed with the data collected by the ALEPH detector at LEP, at centre-of-mass energies between 189 and 209 GeV, corresponding to an integrated luminosity of 628 pb^{-1}. The analysis is based on the detection of isolated and energetic initial state radiation photons, produced in association with chargino pairs whose decay products have little visible energy. The number of candidate events observed is in agreement with that expected from Standard Model background sources. These results are combined with those of other direct searches for charginos, and a lower limit of 88 GeV/c^2 at 95% confidence level is derived for the chargino mass in the case of heavy sfermions, irrespective of the chargino-neutralino mass difference.

Submitted to Physics Letters B

*) See next pages for the list of authors

The ALEPH Collaboration

A. Heister, S. Schael

Physikalisches Institut das RWTH-Aachen, D-52056 Aachen, Germany

R. Barate, R. Brunelière, I. De Bonis, D. Decamp, C. Goy, S. Jezequel, J.-P. Lees, F. Martin, E. Merle, M.-N. Minard, B. Pietrzyk, B. Trocmé

Laboratoire de Physique des Particules (LAPP), IN^{2}P^3-CNRS, F-74019 Annecy-le-Vieux Cedex, France

G. Boix,[25] S. Bravo, M.P. Casado, M. Chmeissani, J.M. Crespo, E. Fernandez, M. Fernandez-Bosman, Ll. Garrido,[15] E. Graugés, J. Lopez, M. Martinez, G. Merino, R. Miquel,[4] Ll.M. Mir,[4] A. Pacheco, D. Paneque, H. Ruiz

Institut de Física d'Altes Energies, Universitat Autònoma de Barcelona, E-08193 Bellaterra (Barcelona), Spain[7]

A. Colaleo, D. Creanza, N. De Filippis, M. de Palma, G. Iaselli, G. Maggi, M. Maggi, S. Nuzzo, A. Ranieri, G. Raso,[24] F. Ruggieri, G. Selvaggi, L. Silvestris, P. Tempesta, A. Tricomi,[3] G. Zito

Dipartimento di Fisica, INFN Sezione di Bari, I-70126 Bari, Italy

X. Huang, J. Lin, Q. Ouyang, T. Wang, Y. Xie, R. Xu, S. Xue, J. Zhang, L. Zhang, W. Zhao

Institute of High Energy Physics, Academia Sinica, Beijing, The People's Republic of China[8]

D. Abbaneo, P. Azzurri, T. Barklow,[30] O. Buchmüller,[30] M. Cattaneo, F. Cerutti, B. Clerbaux, H. Drevermann, R.W. Forty, M. Frank, F. Gianotti, T.C. Greening,[26] J.B. Hansen, J. Harvey, D.E. Hutchcroft, P. Janot, B. Jost, M. Kado,[2] P. Mato, A. Moutoussi, F. Ranjard, L. Rolandi, D. Schlatter, G. Sguazzoni, W. Tejessy, F. Teubert, A. Valassi, I. Videau, J.J. Ward

European Laboratory for Particle Physics (CERN), CH-1211 Geneva 23, Switzerland

F. Badaud, S. Dessagne, A. Falvard,[20] D. Fayolle, P. Gay, J. Jousset, B. Michel, S. Monteil, D. Pallin, J.M. Pascolo, P. Perret

Laboratoire de Physique Corpusculaire, Université Blaise Pascal, IN^{2}P^3-CNRS, Clermont-Ferrand, F-63177 Aubière, France

J.D. Hansen, J.R. Hansen, P.H. Hansen, B.S. Nilsson

Niels Bohr Institute, 2100 Copenhagen, DK-Denmark[9]

A. Kyriakis, C. Markou, E. Simopoulou, A. Vayaki, K. Zachariadou

Nuclear Research Center Demokritos (NRCD), GR-15310 Attiki, Greece

A. Blondel,[12] J.-C. Brient, F. Machefert, A. Rougé, M. Swynghedauw, R. Tanaka H. Videau

Laboratoire de Physique Nucléaire et des Hautes Energies, Ecole Polytechnique, IN^{2}P^3-CNRS, F-91128 Palaiseau Cedex, France

V. Ciulli, E. Focardi, G. Parrini

Dipartimento di Fisica, Università di Firenze, INFN Sezione di Firenze, I-50125 Firenze, Italy

A. Antonelli, M. Antonelli, G. Bencivenni, F. Bossi, P. Campana, G. Capon, V. Chiarella, P. Laurelli, G. Mannocchi,[5] F. Murtas, G.P. Murtas, L. Passalacqua

Laboratori Nazionali dell'INFN (LNF-INFN), I-00044 Frascati, Italy

A. Halley, J. Kennedy, J.G. Lynch, P. Negus, V. O'Shea, A.S. Thompson

Department of Physics and Astronomy, University of Glasgow, Glasgow G12 8QQ,United Kingdom[10]

S. Wasserbaech

Department of Physics, Haverford College, Haverford, PA 19041-1392, U.S.A.

R. Cavanaugh,[33] S. Dhamotharan,[34] C. Geweniger, P. Hanke, V. Hepp, E.E. Kluge, G. Leibenguth, A. Putzer, H. Stenzel, K. Tittel, M. Wunsch[19]

Kirchhoff-Institut für Physik, Universität Heidelberg, D-69120 Heidelberg, Germany[16]

R. Beuselinck, W. Cameron, G. Davies, P.J. Dornan, M. Girone,[1] R.D. Hill, N. Marinelli, J. Nowell, S.A. Rutherford, J.K. Sedgbeer, J.C. Thompson,[14] R. White

Department of Physics, Imperial College, London SW7 2BZ, United Kingdom[10]

V.M. Ghete, P. Girtler, E. Kneringer, D. Kuhn, G. Rudolph

Institut für Experimentalphysik, Universität Innsbruck, A-6020 Innsbruck, Austria[18]

E. Bouhova-Thacker, C.K. Bowdery, D.P. Clarke, G. Ellis, A.J. Finch, F. Foster, G. Hughes, R.W.L. Jones, M.R. Pearson, N.A. Robertson, M. Smizanska

Department of Physics, University of Lancaster, Lancaster LA1 4YB, United Kingdom[10]

O. van der Aa, C. Delaere, V. Lemaitre

Institut de Physique Nucléaire, Département de Physique, Université Catholique de Louvain, 1348 Louvain-la-Neuve, Belgium

U. Blumenschein, F. Hölldorfer, K. Jakobs, F. Kayser, K. Kleinknecht, A.-S. Müller, G. Quast,[6] B. Renk, H.-G. Sander, S. Schmeling, H. Wachsmuth, C. Zeitnitz, T. Ziegler

Institut für Physik, Universität Mainz, D-55099 Mainz, Germany[16]

A. Bonissent, P. Coyle, C. Curtil, A. Ealet, D. Fouchez, P. Payre, A. Tilquin

Centre de Physique des Particules de Marseille, Univ Méditerranée, IN^{2}P^3-CNRS, F-13288 Marseille, France

F. Ragusa

Dipartimento di Fisica, Università di Milano e INFN Sezione di Milano, I-20133 Milano, Italy.

A. David, H. Dietl, G. Ganis,[27] K. Hüttmann, G. Lütjens, W. Männer, H.-G. Moser, R. Settles, G. Wolf

Max-Planck-Institut für Physik, Werner-Heisenberg-Institut, D-80805 München, Germany[16]

J. Boucrot, O. Callot, M. Davier, L. Duflot, J.-F. Grivaz, Ph. Heusse, A. Jacholkowska,[32] C. Loomis, L. Serin, J.-J. Veillet, J.-B. de Vivie de Régie,[28] C. Yuan

Laboratoire de l'Accélérateur Linéaire, Université de Paris-Sud, IN^{2}P^3-CNRS, F-91898 Orsay Cedex, France

G. Bagliesi, T. Boccali, L. Foà, A. Giammanco, A. Giassi, F. Ligabue, A. Messineo, F. Palla, G. Sanguinetti, A. Sciabà, R. Tenchini,[1] A. Venturi,[1] P.G. Verdini

Dipartimento di Fisica dell'Università, INFN Sezione di Pisa, e Scuola Normale Superiore, I-56010 Pisa, Italy

O. Awunor, G.A. Blair, G. Cowan, A. Garcia-Bellido, M.G. Green, L.T. Jones, T. Medcalf, A. Misiejuk, J.A. Strong, P. Teixeira-Dias

Department of Physics, Royal Holloway & Bedford New College, University of London, Egham, Surrey TW20 OEX, United Kingdom[10]

R.W. Clifft, T.R. Edgecock, P.R. Norton, I.R. Tomalin

Particle Physics Dept., Rutherford Appleton Laboratory, Chilton, Didcot, Oxon OX11 OQX, United Kingdom[10]

B. Bloch-Devaux, D. Boumediene, P. Colas, B. Fabbro, E. Lançon, M.-C. Lemaire, E. Locci, P. Perez, J. Rander, J.-F. Renardy, A. Rosowsky, P. Seager,[13] A. Trabelsi,[21] B. Tuchming, B. Vallage

CEA, DAPNIA/Service de Physique des Particules, CE-Saclay, F-91191 Gif-sur-Yvette Cedex, France[17]

N. Konstantinidis, A.M. Litke, G. Taylor

Institute for Particle Physics, University of California at Santa Cruz, Santa Cruz, CA 95064, USA[22]

C.N. Booth, S. Cartwright, F. Combley,[31] P.N. Hodgson, M. Lehto, L.F. Thompson
Department of Physics, University of Sheffield, Sheffield S3 7RH, United Kingdom[10]

K. Affholderbach,[23] A. Böhrer, S. Brandt, C. Grupen, J. Hess, A. Ngac, G. Prange, U. Sieler
Fachbereich Physik, Universität Siegen, D-57068 Siegen, Germany[16]

C. Borean, G. Giannini
Dipartimento di Fisica, Università di Trieste e INFN Sezione di Trieste, I-34127 Trieste, Italy

H. He, J. Putz, J. Rothberg
Experimental Elementary Particle Physics, University of Washington, Seattle, WA 98195 U.S.A.

S.R. Armstrong, K. Berkelman, K. Cranmer, D.P.S. Ferguson, Y. Gao,[29] S. González, O.J. Hayes, H. Hu, S. Jin, J. Kile, P.A. McNamara III, J. Nielsen, Y.B. Pan, J.H. von Wimmersperg-Toeller, W. Wiedenmann, J. Wu, Sau Lan Wu, X. Wu, G. Zobernig
Department of Physics, University of Wisconsin, Madison, WI 53706, USA[11]

G. Dissertori
Institute for Particle Physics, ETH Hönggerberg, 8093 Zürich, Switzerland.

---

[1]Also at CERN, 1211 Geneva 23, Switzerland.
[2]Now at Fermilab, PO Box 500, MS 352, Batavia, IL 60510, USA
[3]Also at Dipartimento di Fisica di Catania and INFN Sezione di Catania, 95129 Catania, Italy.
[4]Now at LBNL, Berkeley, CA 94720, U.S.A.
[5]Also Istituto di Cosmo-Geofisica del C.N.R., Torino, Italy.
[6]Now at Institut für Experimentelle Kernphysik, Universität Karlsruhe, 76128 Karlsruhe, Germany.
[7]Supported by CICYT, Spain.
[8]Supported by the National Science Foundation of China.
[9]Supported by the Danish Natural Science Research Council.
[10]Supported by the UK Particle Physics and Astronomy Research Council.
[11]Supported by the US Department of Energy, grant DE-FG0295-ER40896.
[12]Now at Departement de Physique Corpusculaire, Université de Genève, 1211 Genève 4, Switzerland.
[13]Supported by the Commission of the European Communities, contract ERBFMBICT982874.
[14]Supported by the Leverhulme Trust.
[15]Permanent address: Universitat de Barcelona, 08208 Barcelona, Spain.
[16]Supported by Bundesministerium für Bildung und Forschung, Germany.
[17]Supported by the Direction des Sciences de la Matière, C.E.A.
[18]Supported by the Austrian Ministry for Science and Transport.
[19]Now at SAP AG, 69185 Walldorf, Germany
[20]Now at Groupe d' Astroparticules de Montpellier, Université de Montpellier II, 34095 Montpellier, France.
[21]Now at Département de Physique, Faculté des Sciences de Tunis, 1060 Le Belvédère, Tunisia.
[22]Supported by the US Department of Energy, grant DE-FG03-92ER40689.
[23]Now at Skyguide, Swissair Navigation Services, Geneva, Switzerland.
[24]Also at Dipartimento di Fisica e Tecnologie Relative, Università di Palermo, Palermo, Italy.
[25]Now at McKinsey and Compagny, Avenue Louis Casal 18, 1203 Geneva, Switzerland.
[26]Now at Honeywell, Phoenix AZ, U.S.A.
[27]Now at INFN Sezione di Roma II, Dipartimento di Fisica, Università di Roma Tor Vergata, 00133 Roma, Italy.
[28]Now at Centre de Physique des Particules de Marseille, Univ Méditerranée, F-13288 Marseille, France.
[29]Also at Department of Physics, Tsinghua University, Beijing, The People's Republic of China.
[30]Now at SLAC, Stanford, CA 94309, U.S.A.
[31]Deceased.
[32]Also at Groupe d' Astroparticules de Montpellier, Université de Montpellier II, 34095 Montpellier, France.
[33]Now at University of Florida, Department of Physics, Gainesville, Florida 32611-8440, USA
[34]Now at BNP Paribas, 60325 Frankfurt am Mainz, Germany

1 Introduction

During its last three years of running (1998–2000), the ALEPH detector at LEP collected data from e^+e^- collisions at centre-of-mass energies between 189 and 209 GeV, corresponding to an integrated luminosity of 628 pb^{-1} (Table 1). In this letter, a search is performed on these data for the pair production of charginos, $e^+e^- \to \chi^+\chi^-$, in the framework of supersymmetric models with R-parity conservation and with the lightest neutralino χ as the lightest supersymmetric particle (LSP). In particular, the configuration in which the mass difference Δm between the charginos and the LSP is less than 5 GeV/c^2 is studied.

The small-Δm configuration is possible in the MSSM, the minimal supersymmetric extension of the Standard Model [1], although it requires unusual assumptions to be made for the gaugino mass terms, M_1 and M_2. Indeed, with the usual gaugino-mass unification relation, charginos and neutralinos are nearly mass degenerate only in the deep higgsino region, *i.e.*, for very large M_2 values. However, it happens for more natural values of the MSSM parameters if the gaugino-mass unification assumption is relaxed. It even becomes common in models with anomaly-mediated supersymmetry breaking [2], in which M_1 is naturally much larger than M_2.

Charginos generally decay into the stable LSP and a pair of fermions ($\chi q\bar{q}'$ or $\chi\ell\nu_\ell$). In the small-Δm configuration, three different final state topologies may occur according to the value of Δm.

1. The mass difference, and therefore the phase space available for the chargino decay, is so small that charginos are long-lived. A search for heavy stable charged particles [3, 4] is efficient for this topology.
2. The mass difference is sufficiently large for the chargino decay products to trigger the data acquisition. In this case, the final state is characterized by the large amount of missing energy carried by the invisible LSPs, as searched for in Refs. [5, 6].
3. The mass difference is in between, *i.e.*, large enough for the charginos to decay before leaving the detector, but too small for the decay products to trigger the data acquisition.

The last, intermediate, situation is analysed in this letter. As suggested in Ref. [7], a search for radiative chargino pair production, $e^+e^- \to \gamma\,\chi^+\chi^-$, was performed, where the initial state radiation (ISR) photon is emitted at sufficiently large angle with respect to the incoming beam to be detected, and with sufficiently large energy to activate the trigger system. The relevant topology is therefore an energetic, isolated photon accompanied by a few low-momentum particles from the chargino decays and large missing energy carried by the two neutralinos. This topology has also been searched for by other LEP collaborations [8, 9] with lower energy data.

This letter is organized as follows. In Section 2, the ALEPH detector elements directly related to the ISR photon search are described, followed by a summary of the signal and background simulation in Section 3. The event selection developed for the ISR photon final state is explained in Section 4, the results are presented in Section 5, and their interpretation in the MSSM, combined with those of the other two topological searches mentioned above, is given in Section 6.

Table 1: Integrated luminosities collected between 1997 and 2000, average centre-of-mass energies, and data samples used by the analyses mentioned in the text.

Year	1997	1998	1999				2000			
$\sqrt{s}$ (GeV)	182.7	188.6	191.6	195.5	199.5	201.6	203.2	205.0	206.5	208.0
$\mathcal{L}$ (pb^{-1})	56.8	174.2	28.9	79.8	86.2	42.0	11.6	71.6	126.3	7.3
Stable charginos	Ref. [3]		Ref. [4]							
Missing energy	Ref. [5]						Ref. [6]			
ISR photons	—	This analysis								

2 The ALEPH detector

A complete and detailed description of the ALEPH detector and its performance, as well as of the standard reconstruction and analysis algorithms, can be found in Refs. [10, 11]. Only those items relevant for the final state under study in this letter (an ISR photon accompanied by a few low-momentum particles and substantial missing energy) are described below.

The hermetic electromagnetic calorimeter, a 22-radiation-length-thick sandwich of lead planes and proportional wire chambers with fine readout segmentation, consists of 36 modules, twelve in the barrel and twelve in each endcap. It is used to identify photons and to measure their energies, with a relative resolution of $0.18/\sqrt{E} + 0.009$ (E in GeV), and their positions down to 13° from the beam axis. Unconverted photons are reconstructed as localized energy deposits (clusters) within groups of neighbouring cells in at least two of the three segments in depth of the calorimeter. The longitudinal and transverse distributions of these deposits are required to be consistent with those of an electromagnetic shower. The *impact parameter* with respect to the interaction point is calculated for a given cluster from the barycentres of its energy deposits in each segment. The *compactness* of a cluster is calculated by taking an energy-weighted average of the angle subtended at the interaction point between the barycentre of the whole cluster and the barycentre of its deposit in each segment.

Only those photons with a polar angle such that $|\cos\theta_\gamma| < 0.95$, with an energy in excess of 1 GeV, with an interaction time relative to a beam crossing smaller than 100 ns, with an impact parameter smaller than 80 cm and with a compactness smaller than 1° are considered as ISR photon candidates in this letter. The energy deposits associated with photons from bremsstrahlung of high energy particles in cosmic ray events are rejected by the requirements on interaction time, impact parameter and compactness. Finally, ISR photon candidates are required to be isolated from any reconstructed charged particle by more than 30°.

Charged particles are detected in the central tracking system, which consists of a silicon vertex detector, a cylindrical multiwire inner drift chamber (ITC) and a large time projection chamber (TPC). It is immersed in a 1.5 T axial magnetic field provided by a superconducting solenoidal coil surrounding the electromagnetic calorimeter. Photons traversing the tracking material may convert into electron-positron pairs (in 6% of the cases at normal incidence) and can therefore not be identified as depicted above. To identify these photons, pairs are formed of two oppositely charged particle tracks reconstructed with at least four hits in the TPC and extrapolated to a common vertex; at this position the momenta are computed and the invariant mass of the pair is determined assuming electron masses. Photon conversions are identified if this invariant mass is smaller than $100\,\mathrm{MeV}/c^2$. The same acceptance, energy and isolation criteria are applied as to unconverted photons to define an ISR photon candidate.

Other charged particles in the event are called *good tracks* if they are reconstructed with at least four hits in either the ITC or the TPC, and if they originate from within a cylinder of length 10 cm (for tracks reconstructed with at least four TPC hits) and radius 2 cm (4 cm for tracks reconstructed with no TPC hits) coaxial with the beam and centred at the nominal interaction point.

Global event quantities such as total energy (and therefore missing energy) are determined from an energy-flow algorithm which combines the above measurements supplemented by those of the iron return yoke instrumented as a hadron calorimeter, the surrounding two double layers of muon chambers, and the luminosity monitors, which extend the calorimetric coverage down to 34 mrad. This algorithm provides, in addition, a list of *energy-flow particles*, classified as photons, electrons, muons, and charged and neutral hadrons, which are the basic objects used in the selection presented in this letter.

Finally, use is made of the hadron calorimeter to improve the energy resolution of photons pointing to cracks between modules of the electromagnetic calorimeter. To do so, the energy of any neutral energy-flow particle is added to that of an ISR photon candidate if it is within 11.5° of the photon direction.

The trigger condition relevant for this analysis consists of a deposit of at least 1 GeV (2.3 GeV) in any single module of the barrel (the endcaps) of the electromagnetic calorimeter. This trigger is fully efficient for ISR photons within the acceptance of the present search.

3 Event simulation

Background events expected from Standard Model processes were generated with statistics corresponding to at least 20 times the integrated luminosity of the data. The event generators used for the present analysis are listed in Table 2.

Signal events were simulated with the program SUSYGEN [17]. Charginos were produced with masses ranging from $45\,\mathrm{GeV}/c^2$ up to the kinematic limit, for mass differences with the LSP between m_{e} and $5\,\mathrm{GeV}/c^2$ and with proper decay length $\lambda = c\tau$ up to 80 cm. Hadronic decays were modelled as suggested in Ref. [18]. For $\Delta m < 2\,\mathrm{GeV}/c^2$, the model of Ref. [19] was used for the spectral functions, with parameters tuned to agree with the measured hadronic τ decays [20]. In this case, chargino decays to $\mathrm{e}\nu_{\mathrm{e}}\chi$, $\mu\nu_\mu\chi$ and $n\pi\,\chi$ ($n = 1, 2, 3$) were simulated. For larger Δm values, the Lund fragmentation scheme was applied, as implemented in SUSYGEN. Initial state radiation was simulated according to the treatment described in Ref. [21].

Table 2: Standard Model background processes and the generators used to simulate them in the present analysis.

Standard Model processes	Generators
$\mathrm{e^+e^-} \to \gamma(\gamma)\nu\bar{\nu}$	KORALZ [12]
$\mathrm{e^+e^-} \to \mathrm{e^+e^-}$	BHWIDE [13]
$\mathrm{e^+e^-} \to \mu^+\mu^-,\ \tau^+\tau^-$	KORALZ
$\mathrm{e^+e^-} \to \mathrm{q\bar{q}}$	KORALZ
$\mathrm{e^+e^-} \to \mathrm{W^+W^-}$	KORALW [14]
$\mathrm{e^+e^-} \to \mathrm{We}\nu$, ZZ, $\mathrm{Ze^+e^-}$, $\mathrm{Z}\nu\bar{\nu}$	PYTHIA [15]
$\gamma\gamma \to \mathrm{e^+e^-},\ \mu^+\mu^-,\ \tau^+\tau^-$	PHOT02 [16]
$\gamma\gamma \to \mathrm{q\bar{q}}$	PHOT02

4 Event selection

Events are selected if they contain at least one ISR photon candidate (a calorimeter photon or a photon conversion) reconstructed with transverse momentum p_T^γ with respect to the beam axis greater than $0.035\sqrt{s}$. This requirement effectively rejects the background from $\gamma\gamma$ interactions, further reduced by requiring that no energy be detected within 14° of the beam axis. This last cut is also useful to suppress background from Bhabha scattering.

At least two charged particle tracks with a minimum of four ITC or four TPC hits are required, and at most ten good tracks. The latter cut efficiently reduces the backgrounds from hadronic two- and four-fermion processes. In events from $\mathrm{e^+e^-} \to \gamma\gamma\nu\bar{\nu}$, a photon may convert at the ITC/TPC boundary, but fail to be identified by the criteria of Section 2 while still being reconstructed as two charged particles. This background is rejected by requiring that at least one track be reconstructed with at least one ITC hit.

Advantage is taken of the characteristic kinematic features of radiative chargino pair production. The ISR photon energy is required to be smaller than the maximum energy allowed in the process $\mathrm{e^+e^-} \to \gamma\chi^+\chi^-$, and the leading charged particle momentum is limited to the maximum allowed chargino momentum. The mass recoiling against the ISR photon must be larger than $100\,\mathrm{GeV}/c^2$. Sliding upper cuts are applied to the missing transverse momentum and to the energy of the chargino decay products as a function of the hypothetical chargino mass and mass difference with the LSP; these cuts were determined from the simulation of promptly decaying charginos.

5 Results and systematic uncertainties

The selection efficiency is shown in Fig. 1a as a function of the generated p_{T}^{γ}. For p_{T}^{γ} in excess of 15 GeV/c, the selection efficiency is above 45%. The photon identification criteria described in Section 2 (acceptance, reconstruction, isolation, timing and pointing) are responsible for an efficiency loss of 40%, and the remaining loss is due to the event selection of Section 4. Because the p_{T}^{γ} spectrum is peaked at small values, the total selection efficiency is at most 3%.

The dependence of the selection efficiency on p_{T}^{γ} is qualitatively identical for all chargino masses studied, but the absolute efficiency level depends also on the chargino decay length and on the available phase space $Q = \Delta m - \sum_i m_i$, where the sum runs over the chargino decay products.

For instance, the efficiency for promptly-decaying charginos with mass 87 GeV/c^2 is shown in Fig. 1b as a function of Δm for the single pion final state, and is compared to that for charginos with a proper decay length λ of 30 cm. The higher efficiency for larger decay lengths for very low Q is due to the detection of the chargino tracks. For the same λ, at larger Δm, the chargino detection efficiency is lower with respect to the case $\lambda = 0$ because of the cuts on the reconstructed energy in addition to the photon and on the total visible momentum of the event. The dependence on the proper decay length is displayed in Fig. 1c, for $\Delta m = 140$, 150 and 200 MeV/c^2.

The dependence of the absolute efficiency on the chargino mass (through its effect on the p_{T}^{γ} spectrum) is shown in Fig. 1d, for three different final states (electron, muon and single pion), for fixed Q values and $\lambda = 0$. At the same Q, the decay into an electron is reconstructed less efficiently than the decay into a muon due to the mass of the final state lepton, and the efficiency for the three-body decays is smaller than for the two-body decay to a single pion.

The photon spectrum is also strongly dependent on the field content of the chargino which is different in various regions of the MSSM parameter space. Initial state radiation is enhanced in the gaugino region due to the relative contribution of the s-channel Z exchange. All the plots shown in Fig. 1 were derived in the gaugino region.

The efficiency includes a $(-5 \pm 1)\%$ correction for the loss due to the cut on the energy measured within 14° of the beam axis, caused by beam-related background in the forward calorimeters. This correction is determined with events triggered at random beam crossings.

A systematic uncertainty of 0.6% on the efficiency, related to the algorithm of photon reconstruction, is taken into account as described in Ref. [22]. The uncertainty on the number of converted photons is estimated to change the total selection efficiency by up to 0.3%.

Systematic uncertainties from the ISR photon simulation are assessed by comparing the ISR photon transverse momentum spectrum as predicted by the SUSYGEN and KORALZ programs. The distributions obtained from KORALZ for the mass recoiling against the photon and for the polar angle of the photon in single photon events are in agreement with data [22]. The systematic uncertainty on the efficiency of the present selection is estimated by integrating the possible discrepancy of the p_T^γ distributions between the two generators over the allowed range, which depends on the chargino mass. The systematic uncertainty obtained is at most 10%.

The systematic error on the efficiency due to the limited statistics of the simulated samples is about 3%. The total systematic uncertainty on the selection efficiency is 10%, obtained by adding in quadrature the individual contributions.

The numbers of events observed are in agreement with those expected from Standard Model background sources, dominated by $e^+e^- \rightarrow \tau^+\tau^-$, $\gamma\gamma \rightarrow \tau^+\tau^-$ and $e^+e^- \rightarrow \gamma(\gamma)\nu\bar{\nu}$, as shown in Table 3 for several chargino masses and mass differences. These numbers are displayed in Fig. 2 in the $(m_{\chi^\pm}, \Delta m)$ plane. A candidate event that contributes up to $m_{\chi^\pm} = 84$ GeV/c^2, independent of Δm, is shown in Fig. 3.

Table 3: Numbers of events observed and expected from Standard Model background sources for $m_{\chi^\pm} > 50,\ 65,\ 85$ GeV/c^2 and $\Delta m < 2,\ 1,\ 0.3$ GeV/c^2, respectively. The main contributions to the expected background are also reported.

$\sqrt{s} = 189$–209 GeV		Data	Background					
$m_{\chi^\pm}$	Δm	N_{obs}	$e^+e^- \rightarrow \gamma(\gamma)\nu\bar{\nu}$	$\gamma\gamma \rightarrow \tau^+\tau^-$	$\gamma\gamma \rightarrow e^+e^-$	$e^+e^- \rightarrow \tau^+\tau^-$	four fermions	N_{exp}
> 50	< 2	13	1.2	2.0	0.3	3.8	1.3	9.0
> 65	< 1	5	0.7	1.8	0.3	1.7	0.6	5.4
> 85	< 0.3	1	0.6	1.4	0	0.5	0	2.9

6 Interpretation in the MSSM

In order to provide complete coverage of all possible chargino decay lengths, the results of the present analysis, hereafter called *the ISR analysis*, were combined with those of the search for heavy stable charged particles [3, 4], needed for very small Δm values, and the standard missing-energy search [5, 6], efficient for $\Delta m \geq 3\,\text{GeV}/c^2$. No background subtraction was performed and systematic uncertainties were taken into account according to Ref. [23].

In the MSSM, and in the absence of the assumption of gaugino-mass unification, four parameters are to be considered in the gaugino sector: the soft-breaking gaugino mass terms, M_1 and M_2; the Higgs mixing term, μ; and the ratio of the two Higgs-doublet vacuum expectation values, $\tan\beta$. To determine 95% confidence level (C.L.) excluded regions in the $(m_{\chi^\pm}, \Delta m)$ plane, a broad scan of these parameters was performed: $1 < \tan\beta < 300$, $|\mu| < 1\,\text{TeV}/c^2$, $M_2 < 250\,\text{TeV}/c^2$, and M_1 chosen so as to cover the range $\Delta m < 5\,\text{GeV}/c^2$.

The regime in which all sfermion masses are very large is considered first. In this case, the chargino production cross section depends only on the four above-mentioned parameters, and charginos generically decay via $\chi^\pm \to \chi \text{W}^{\pm *}$.

In the gaugino region ($M_2 \ll |\mu|$), it is possible to fine-tune $\tan\beta$ to make the $\chi^\pm \chi \text{W}^\pm$ coupling vanish, in which case the chargino decay length increases substantially, even for large Δm values. As a result, the ISR analysis is efficient independently of $\tan\beta$ only over a limited range of Δm, the extent of which depends on the $\chi^+ \tilde{\text{f}}\bar{\text{f}}'$ couplings. This effect was quantitatively investigated under the assumption of a universal sfermion mass term m_0. The dependence on $\tan\beta$ of the chargino decay length is shown for $m_{\chi^\pm} = 71\,\text{GeV}/c^2$ in Fig. 4a, for $m_0 = 500\,\text{GeV}/c^2$ and for various Δm values. The exclusion domain in the $(m_{\chi^\pm}, \Delta m)$ plane derived at $m_0 = 500\,\text{GeV}/c^2$ and fixed $\tan\beta = 21$ (which corresponds to the maximum decay length for a chargino mass of $88\,\text{GeV}/c^2$) is shown in Fig. 4b; the ISR analysis covers the gap between the standard missing energy search and the stable particle analysis. Results independent of $\tan\beta$ are also shown in Fig. 5 for $m_0 = 500\,\text{GeV}/c^2$. The standard missing energy search excludes Δm values larger than $\sim 2.3\,\text{GeV}/c^2$, and the ISR analysis Δm values down to 1 to $1.5\,\text{GeV}/c^2$. The search for heavy stable charged particles is fully efficient in a parameter-independent way only for $\Delta m < m_\pi$, but a combination with the ISR analysis allows the exclusion of the intermediate Δm range to be achieved, independently of $\tan\beta$. In the end, a 95% C.L. lower limit on the chargino mass of $88\,\text{GeV}/c^2$ is set in the gaugino region for heavy sfermions (*i.e.,* for sfermion masses, or m_0, larger than a few hundred GeV/c^2).

In the Higgsino region ($|\mu| \ll M_2$), the chargino production cross section is smaller than in the gaugino region, but this effect is compensated by a generically larger chargino decay length, together with a reduced influence of $\tan\beta$. As a result, the ISR analysis on its own excludes a region larger than in the former case, namely Δm between $150\,\text{MeV}/c^2$ and $3\,\text{GeV}/c^2$ (Fig. 6), with only a slight dependence on m_0. The combination of the three analyses allows a lower limit on the chargino mass to be set at $88\,\text{GeV}/c^2$ in the Higgsino region. It was checked with a scan on the μ parameter that the $88\,\text{GeV}/c^2$ mass limit, obtained in the gaugino and Higgsino regions, is generally valid for large sfermion masses.

For small enough sfermion (most importantly slepton) masses, the chargino lifetime can be substantially reduced, even for very small Δm values. As a result, the search for heavy stable particles loses efficiency for some parameter configurations as soon as $\Delta m > m_\text{e}$, while the ISR analysis is inefficient for such small Δm values. Therefore, the only completely general chargino mass limit is $m_\text{Z}/2$, as derived from the Z width measurement at LEP 1 [24].

In a more constrained version of the MSSM, namely with gaugino- and sfermion-mass unification, charginos degenerate in mass with the lightest neutralino are only possible in the deep Higgsino region. For such large M_2 values, all sfermions are heavy. An absolute chargino mass lower limit of $88\,\mathrm{GeV}/c^2$ therefore holds within this framework.

7 Conclusions

A search for charginos nearly mass degenerate with the lightest neutralino has been performed using data collected by the ALEPH detector at LEP at centre-of-mass energies between 189 and 209 GeV. No excess of candidate events with respect to Standard Model background predictions was found.

The results have been interpreted in terms of exclusion limits in the framework of the MSSM; in the heavy sfermion scenario the absolute 95% C.L. chargino mass lower limit is 88 GeV/c^2 for any $\tan\beta$, irrespective of the chargino field content.

In the light sfermion scenario, no Δm-independent limit on the chargino mass is set from direct searches. Chargino masses up to $m_{\mathrm{Z}}/2$ are excluded, indirectly, from the measurement of the Z total width at LEP 1.

Acknowledgements

We wish to congratulate our colleagues from the accelerator divisions for the successful operation of LEP at high energies. We would also like to express our gratitude to the engineers and support people at our home institutes without whom this work would not have been possible. Those of us from non-member states wish to thank CERN for its hospitality and support.

References

[1] H.P. Nilles, Phys. Rep. **C 110** (1984) 1;
H.E. Haber and G.L. Kane, Phys. Rep. **C 117** (1985) 75;
R. Barbieri, Riv. Nuovo Cimento **11** (1988) 1.

[2] L. Randall and R. Sundrum, Nucl. Phys. **B 557** (1999) 79;
T. Gherghetta, G.F. Giudice and J. D. Wells, Nucl. Phys. **B 559** (1999) 27.

[3] The ALEPH Coll., *"Search for pair-production of long-lived heavy charged particles in e^+e^- annihilation"*, Phys. Lett. **B 405** (1997) 379;
"Search for gauge mediated SUSY breaking topologies at $\sqrt{s} \sim 189\,GeV$", Eur. Phys. J. **C 16** (2000) 1.

[4] The ALEPH Coll., *"Search for Gauge Mediated SUSY Breaking topologies in e^+e^- collisions at centre-of-mass energies up to 209 GeV"*, CERN-EP/2002–xxx, to be submitted to Eur. Phys. J. **C**.

[5] The ALEPH Coll., *"Search for charginos and neutralinos in* e^+e^- *collisions at centre-of-mass energies near 183 GeV and constraints on the MSSM parameter space"*, Eur. Phys. J. **C 11** (1999) 193;
"Search for supersymmetric particles in e^+e^- *collisions at* $\sqrt{s}$ *up to 202 GeV and mass limit for the lightest neutralino"*, Phys. Lett. **B 499** (2001) 67.

[6] The ALEPH Coll., *"Search for charginos and neutralinos in* e^+e^- *collisions at* $\sqrt{s}$ *up to 208 GeV and mass limit for the lightest neutralino"*, ALEPH-CONF 2001–009.

[7] C.H. Chen, M. Drees, and J.F. Gunion, Phys. Rev. Lett. **76** (1996) 2002.

[8] The DELPHI Coll., *"Search for charginos nearly mass-degenerate with the lightest neutralino"*, Eur. Phys. J. **C 11** (1999) 1;
"Update of the search for charginos nearly mass-degenerate with the lightest neutralino", Phys. Lett. **B 485** (2000) 95.

[9] The L3 Coll., *"Search for charginos with a small mass difference to the lightest supersymmetric particle at* $\sqrt{s} = 189$ *GeV"*, Phys. Lett. **B 482** (2000) 31.

[10] The ALEPH Coll., *"ALEPH: A detector for electron positron annihilation at LEP"*, Nucl. Instrum. and Methods **A 294** (1990) 121.

[11] The ALEPH Coll., *"Performance of the ALEPH detector at LEP"*, Nucl. Instrum. and Methods **A 360** (1995) 121.

[12] S. Jadach, B.F.L. Ward and Z. Was, *"*`KORALZ` *version 4.2"*, Comput. Phys. Commun. **79** (1994) 503.

[13] S. Jadach, W. Placzec and B.F.L. Ward, Phys. Lett. **B 390** (1997) 298.

[14] M. Skrypek, S. Jadach, W. Placzek, and Z. Was, *"*`KORALW` *version 1.21"*, Comput. Phys. Commun. **94** (1996) 216.

[15] T. Sjöstrand, *"PYTHIA 5.7 and JETSET 7.4 Physics and Manual"*, CERN-TH/7112/93 (1993), revised August 1995;
T. Sjöstrand, Comput. Phys. Commun. **82** (1994) 74.

[16] J.A.M. Vermaseren in *"Proceedings of the* IV^{th} *International Workshop on Gamma Gamma Interactions"*, Eds G. Cochard and P. Kessler, Springer Verlag, (1980);
The ALEPH Coll., *"An experimental study of* $\gamma\gamma \to$ *hadrons at LEP"*, Phys. Lett. **B 313** (1993) 509.

[17] S. Katsanevas and P. Morawitz, *"*`SUSYGEN` *version 2.2"*, Comput. Phys. Commun. **122** (1998) 227.

[18] C.H. Chen, M. Drees and J.F. Gunion, Phys. Rev. **D 55** (1997) 330; and erratum, Phys. Rev. Lett. **82** (1999) 3192.

[19] J.H. Kühn and A. Santamaria, Z. Phys. **C 48** (1990) 445.

[20] The ALEPH Coll., *"Measurement of the spectral functions of vector current hadronic τ decays"*, Z. Phys. **C 76** (1997) 15;
"Measurement of the spectral functions of axial-vector hadronic τ decays and determination of $\alpha_s(M_\tau^2)$", Eur. Phys. J. **C 4** (1998) 409.

[21] F.A. Berends and R. Kleiss, Nucl. Phys. **B 260** (1985) 32.

[22] The ALEPH Coll., *"Single- and multi-photon production in e^+e^- collisions at a centre-of-mass energy between 188.6 and 201.6 GeV"*, ALEPH-CONF 2000-005;
"Single- and multi-photon production in e^+e^- collisions at centre-of-mass energies between 189 and 207 GeV", paper in preparation.

[23] R.D. Cousins and V.L. Highland, Nucl. Instrum. and Methods **A 320** (1992) 331.

[24] The LEP Collaborations ALEPH, DELPHI, L3, OPAL, the LEP Electroweak Working Group and the SLD Heavy Flavour and Electroweak Working Groups, *"A combination of Preliminary Electroweak Measurements and Constraints on the Standard Model"*, CERN-EP/2001-098.

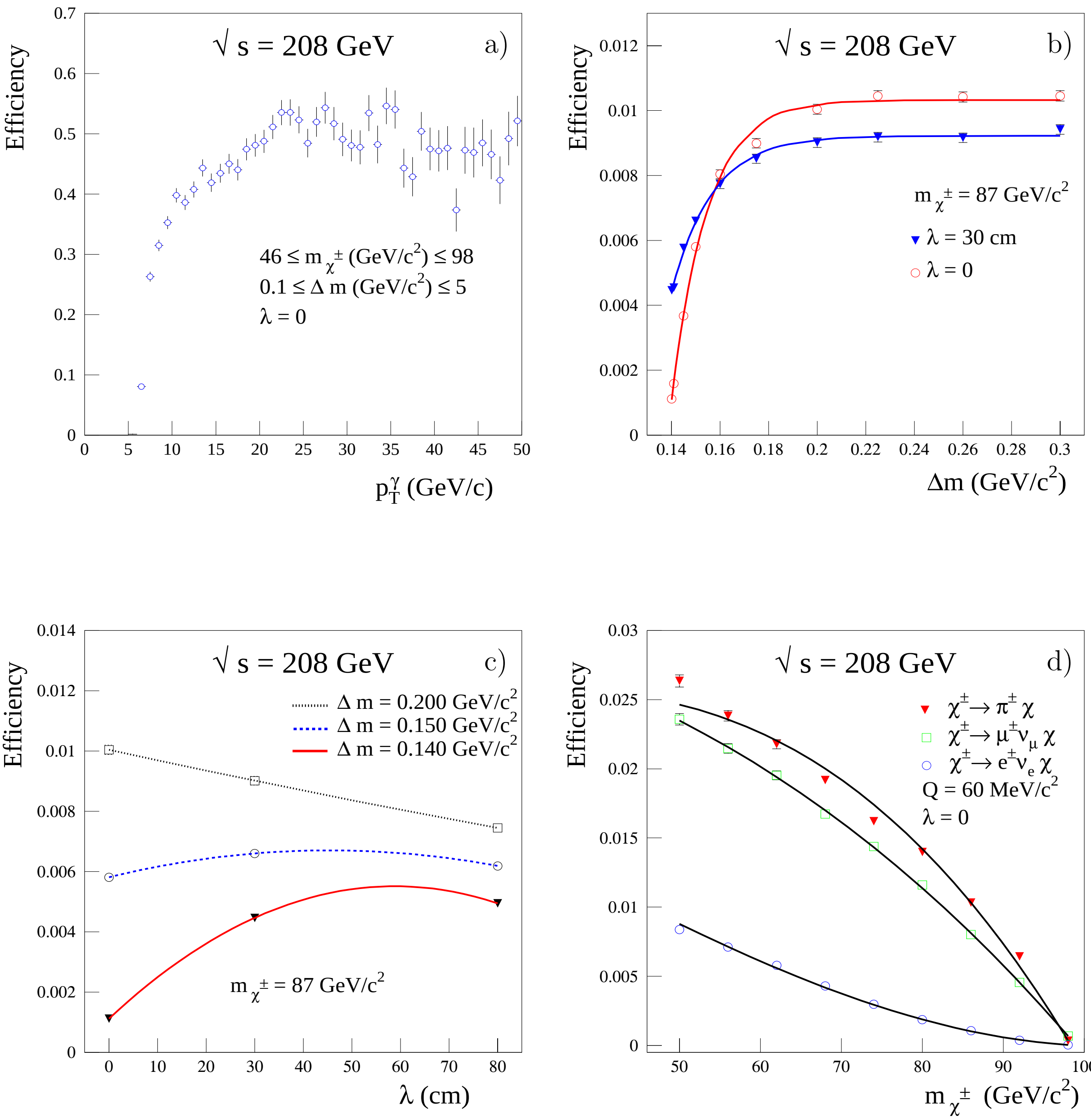

Figure 1: a) Selection efficiency as a function of the generated transverse momentum of the ISR photon produced in association with charginos decaying promptly with masses between 46 and 98 GeV/c^2, Δm between 0.1 and 5 GeV/c^2 at $\sqrt{s} = 208$ GeV. b) Signal efficiency as a function of Δm at $\sqrt{s} = 208$ GeV, $m_{\chi^\pm} = 87\,\mathrm{GeV}/c^2$ and $\lambda = 0$, 30 cm for the single-pion final state. c) Signal efficiency as a function of λ at $\sqrt{s} = 208$ GeV, $m_{\chi^\pm} = 87\,\mathrm{GeV}/c^2$ and $\Delta m = 0.14$, 0.15, 0.2 GeV/c^2. d) Signal efficiency as a function of the chargino mass at $\sqrt{s} = 208$ GeV for $Q = 60\,\mathrm{MeV}/c^2$, $\lambda = 0$, for the single-pion and leptonic final states.

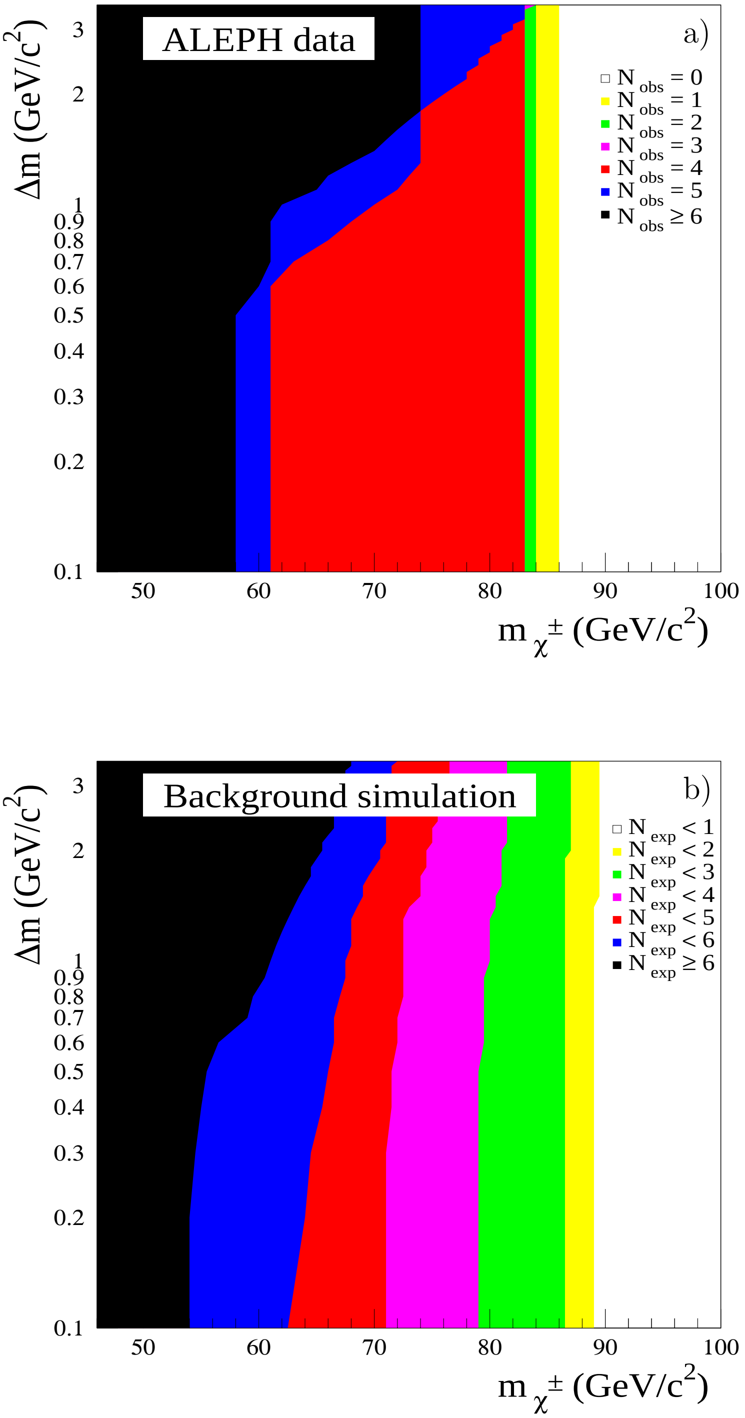

Figure 2: Number of events a) observed and b) expected from standard background sources in the $(m_{\chi^\pm}, \Delta m)$ plane. The number of events decreases for large chargino masses or low Δm due to the tightening of the cuts on the transverse missing momentum and on the total energy not associated with the reconstructed photons. No events compatible with $m_{\chi^\pm} > 86\,\mathrm{GeV}/c^2$ are observed in the data.

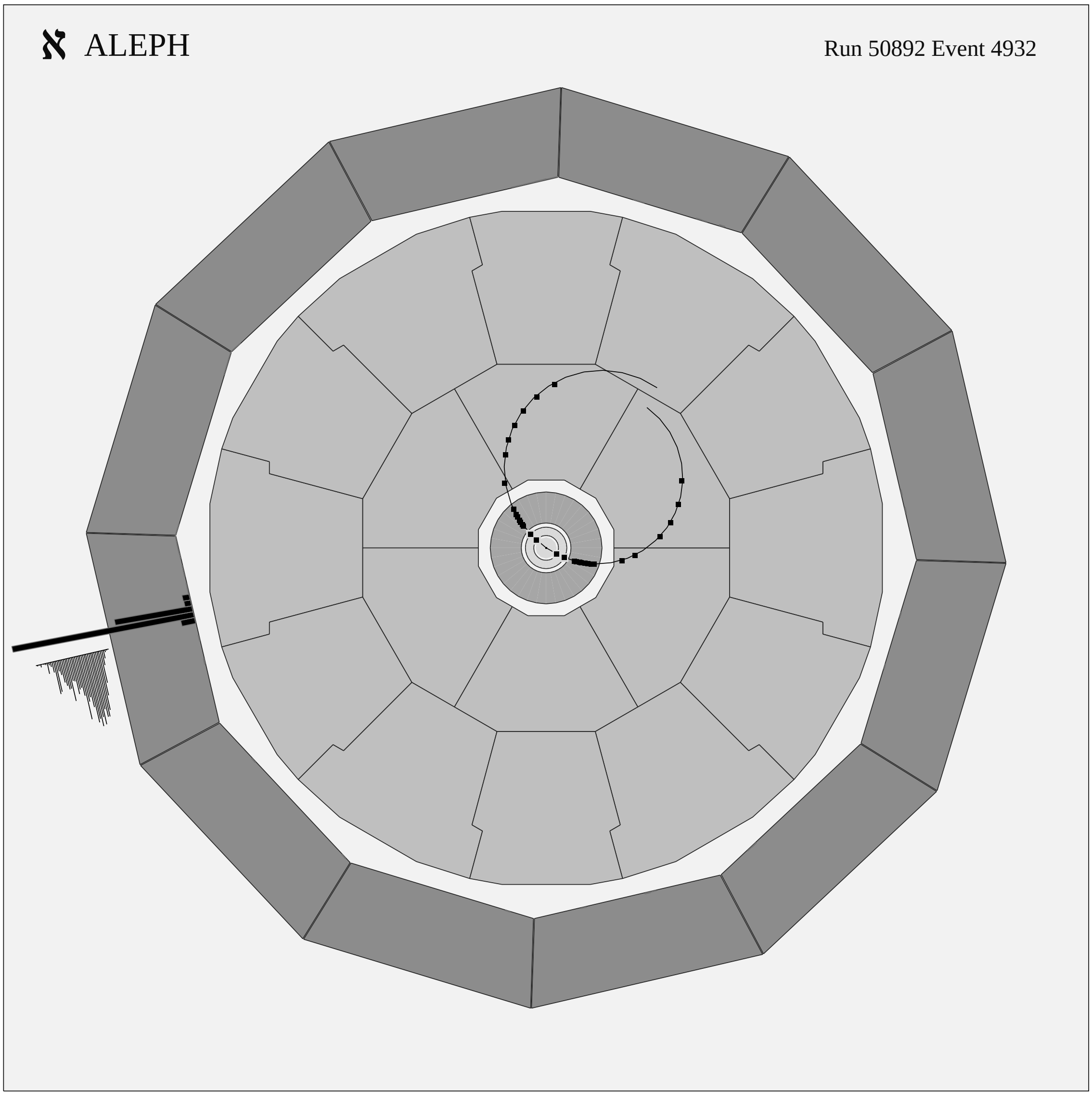

Figure 3: Candidate event at $\sqrt{s} = 195.5\,\mathrm{GeV}$ which contributes to the range $m_{\chi^\pm} \leq 84\ \mathrm{GeV}/c^2$. The reconstructed photon energy is $21\,\mathrm{GeV}$.

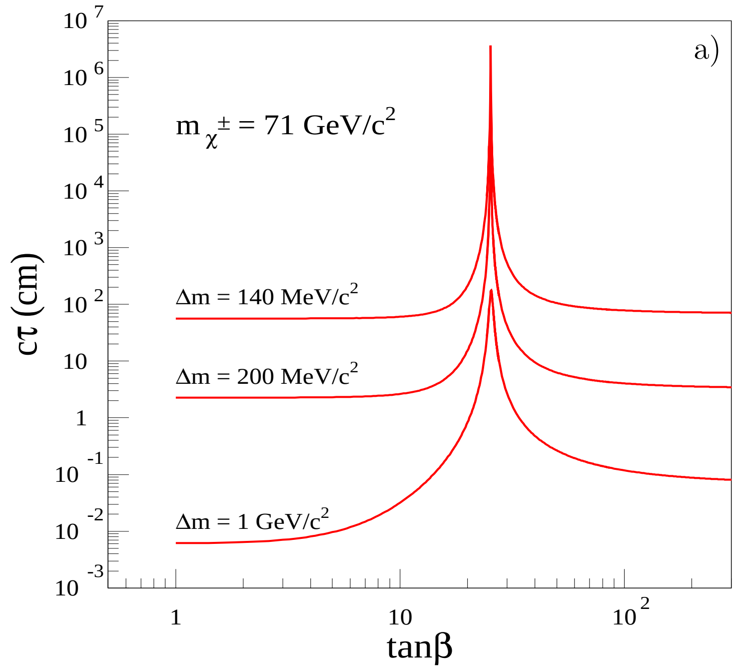

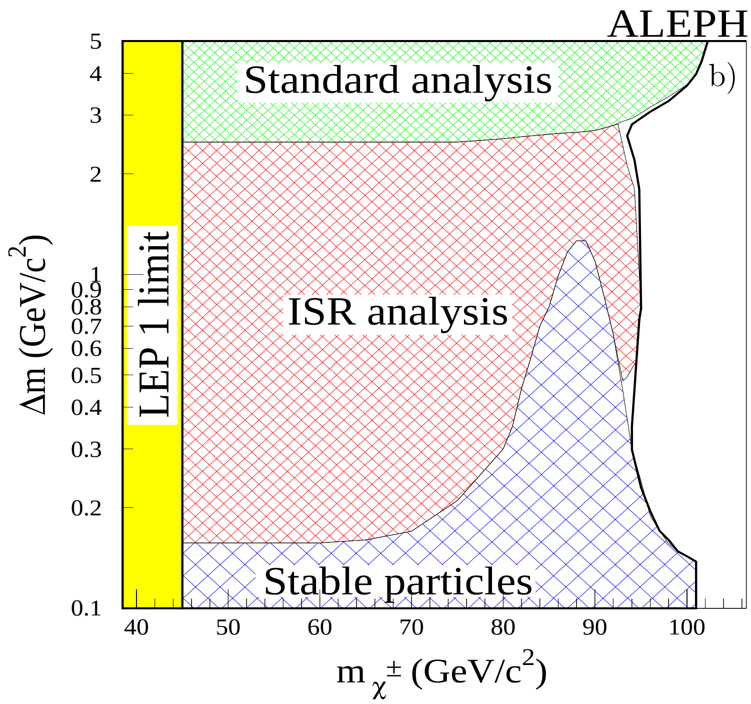

Figure 4: a) Chargino proper decay length as a function of $\tan\beta$ for $m_{\chi^\pm} = 71\,\mathrm{GeV}/c^2$, for $m_0 = 500\,\mathrm{GeV}/c^2$ and for $\Delta m = 140,\ 200,\ 1000\ \mathrm{MeV}/c^2$. b) Exclusion region in the $(m_{\chi^\pm}, \Delta m)$ plane at 95% C.L., in the large scalar mass scenario ($m_0 = 500\,\mathrm{GeV}/c^2$) and in the gaugino region, for $\tan\beta = 21$. The top area is excluded by the standard missing energy chargino selection [5, 6] while the bottom area is excluded by the stable particle search [3, 4]. The ISR analysis covers the intermediate area. The region excluded by the combination of the three analyses is bounded by the bold curve. The region excluded at LEP 1 is also shown.

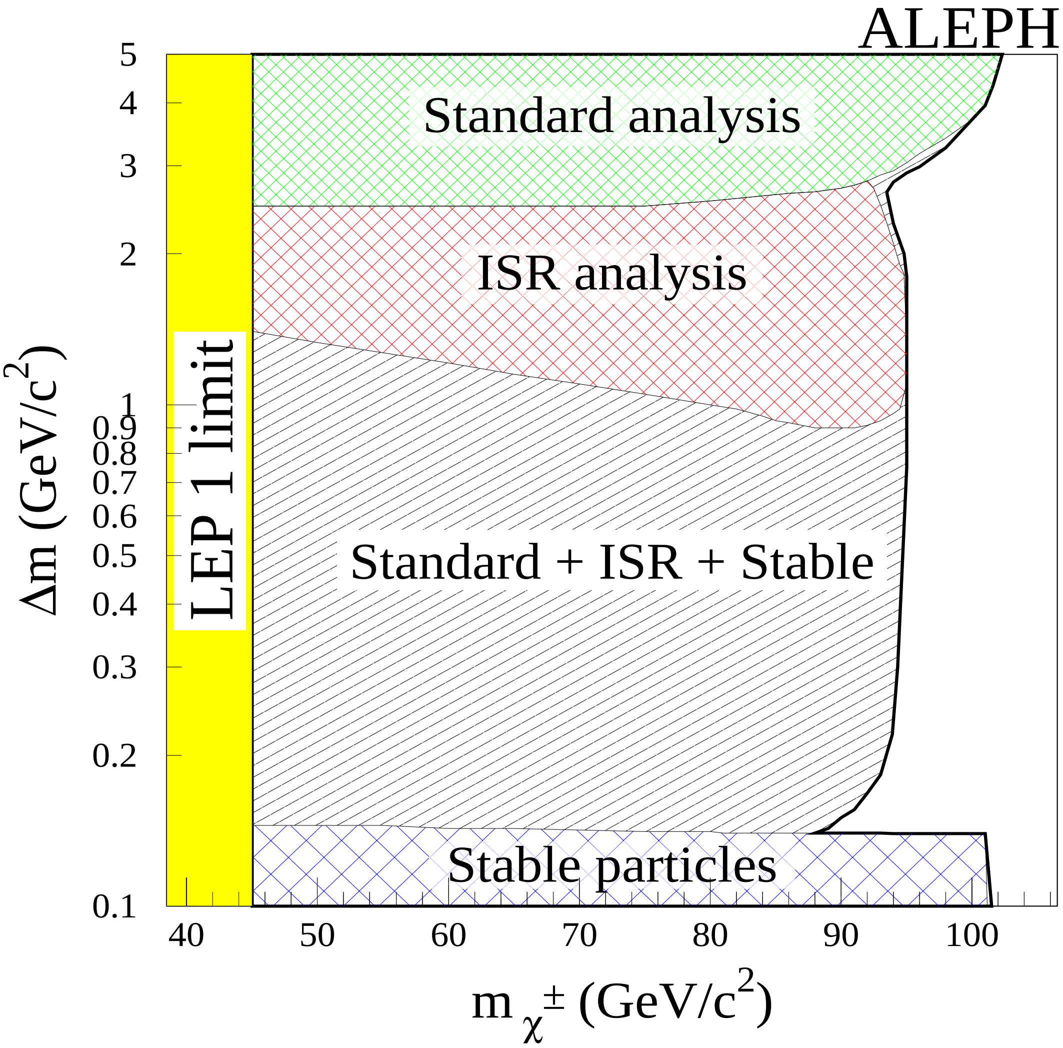

Figure 5: Excluded region in the $(m_{\chi^\pm}, \Delta m)$ plane at 95% C.L., in the large scalar mass scenario ($m_0 = 500\,\mathrm{GeV}/c^2$) and in the gaugino region, independently of $\tan\beta$. The top area is excluded by the standard missing energy chargino selection [5, 6] while the bottom area is excluded by the stable particle search [3, 4]. The ISR analysis provides the exclusion for $\Delta m \sim 1$ to $2.5\,\mathrm{GeV}/c^2$. The remaining Δm region is excluded by the combination of the ISR analysis and of the stable particle search. The region excluded by the combination of the three analyses is bounded by the bold curve. The region excluded at LEP 1 is also shown.

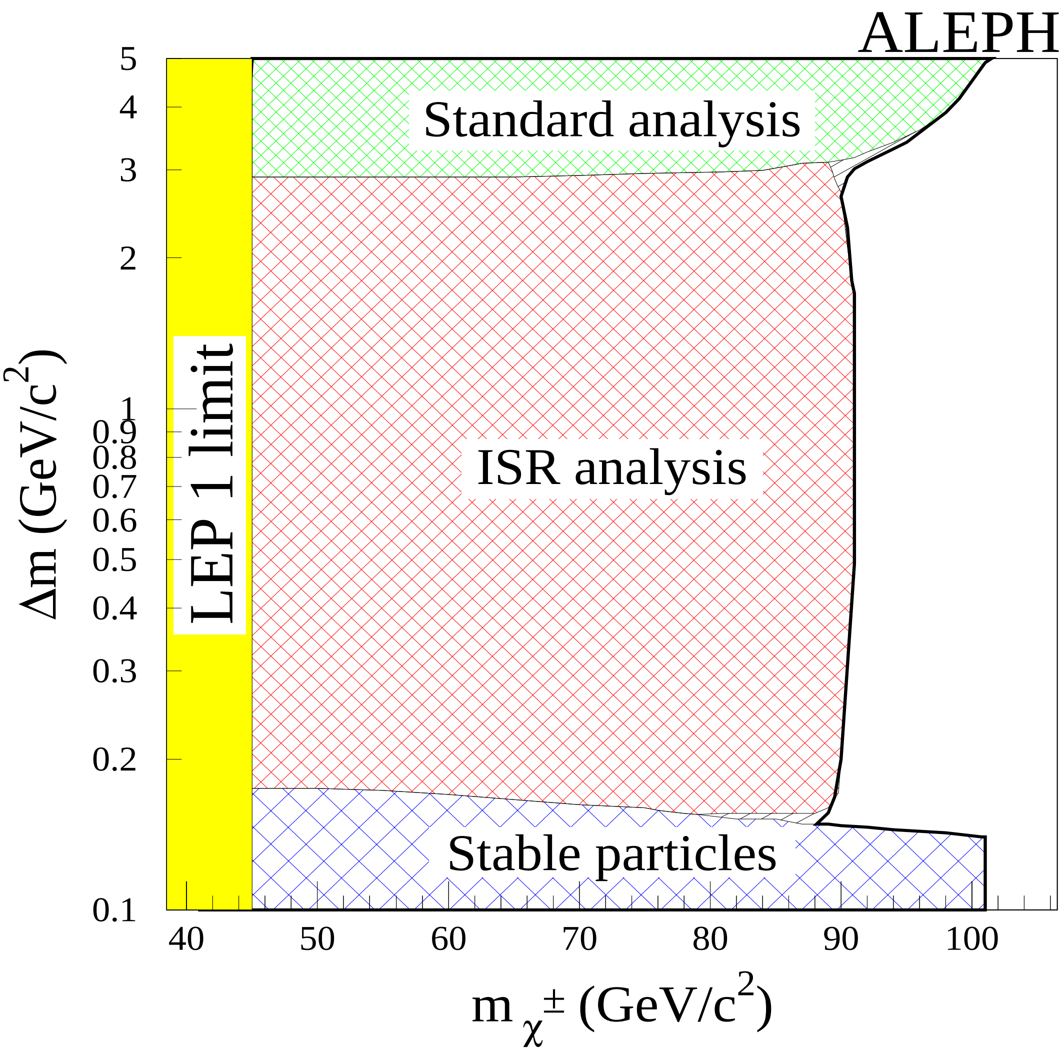

Figure 6: Excluded region in the $(m_{\chi^\pm}, \Delta m)$ plane at 95% C.L., in the large scalar mass scenario ($m_0 = 500\,\mathrm{GeV}/c^2$) and in the Higgsino region, independently of $\tan\beta$. The top area is excluded by the standard missing energy chargino selection [5, 6] while the bottom area is excluded by the stable particle search [3, 4]. The intermediate area is excluded by the ISR analysis. The region excluded by the combination of the three analyses is bounded by the bold curve. The region excluded at LEP 1 is also shown.